iScience

CellPress
OPEN ACCESS

Article

Cbl-b restrains priming of pathogenic Th17 cells via the inhibition of IL-6 production by macrophages

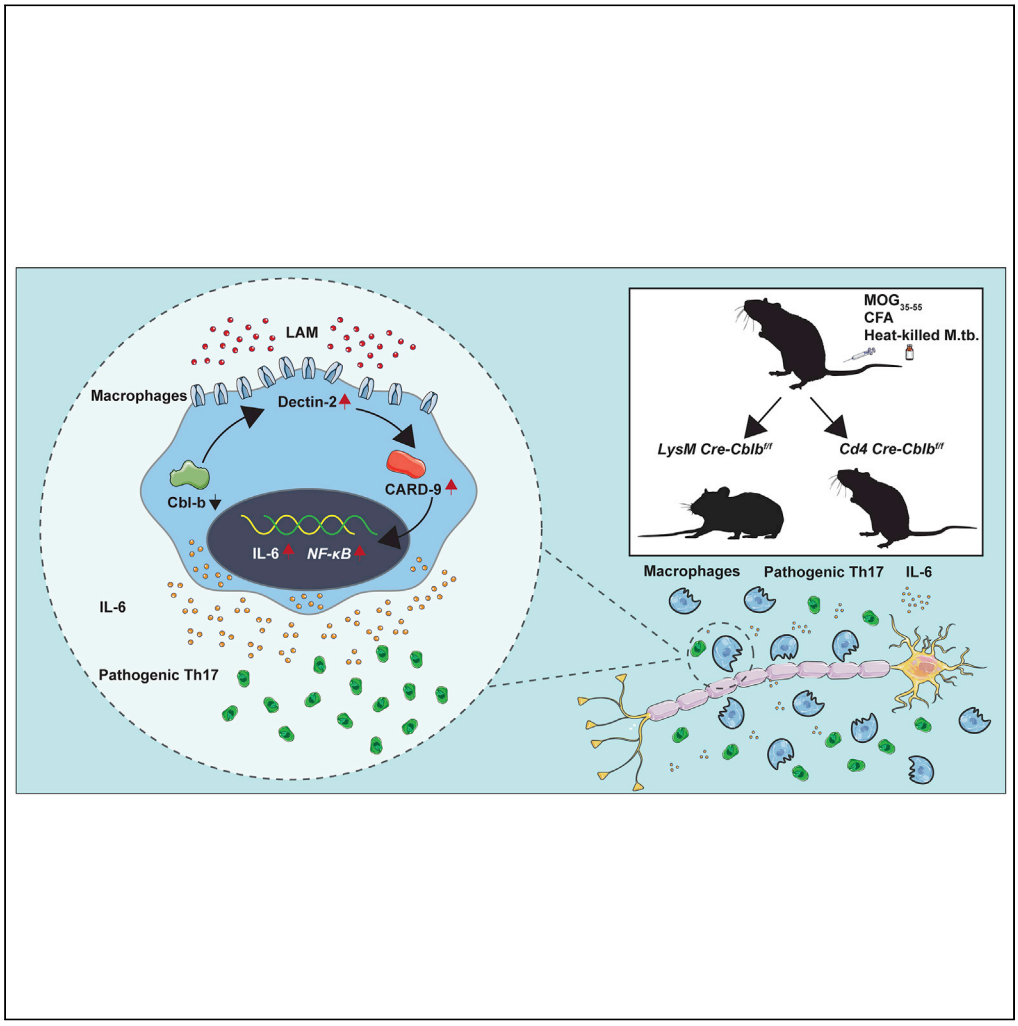

Qiuming Zeng, Na Tang, Yilei Ma, ..., Huan Yang, Matthew C. O'Brien, Jian Zhang

jian-zhang@uiowa.edu

Highlights

E3 ubiquitin ligase Cbl-b inhibits EAE disease progression

Cbl-b dampens pathogenic Th17 response via inhibiting macrophage-derived IL-6

Cbl-b controls macrophage-derived IL-6 via a CARD9-dependent manner

Zeng et al., iScience 25, 105151
October 21, 2022
https://doi.org/10.1016/j.isci.2022.105151

iScience

CellPress
OPEN ACCESS

Article

Cbl-b restrains priming of pathogenic Th17 cells via the inhibition of IL-6 production by macrophages

Qiuming Zeng,[1,2,3] Na Tang,[1,2] Yilei Ma,[1] Hui Guo,[1,2] Yixia Zhao,[2,4] Rong Tang,[2,5] Chengkai Yan,[1] Song Ouyang,[2,6] Wallace Y. Langdon,[7] Huan Yang,[3] Matthew C. O'Brien,[1] and Jian Zhang[1,2,8,*]

SUMMARY

E3 ubiquitin ligase Cbl-b is involved in the maintenance of a balance between immunity and tolerance. Mice lacking Cbl-b are highly susceptible to experimental autoimmune encephalomyelitis (EAE), a Th17-mediated autoimmune disease. However, how Cbl-b regulates Th17 cell responses remains unclear. In this study, utilizing adoptive transfer and cell type-specific *Cblb* knockout strains, we show that Cbl-b expression in macrophages, but not T cells or dendritic cells (DCs), restrains the generation of pathogenic Th17 cells and the development of EAE. Cbl-b inhibits IL-6 production by macrophages that is induced by signaling from CARD9-dependent C-type lectin receptor (CLR) pathways, which directs T cells to generate pathogenic Th17 cells. Therefore, our data unveil a previously unappreciated function for Cbl-b in the regulation of pathogenic Th17 responses.

INTRODUCTION

Casitas-B-lineage lymphoma protein-b (Cbl-b), a Cbl family E3 ubiquitin ligase, encompasses multiple functional domains, including a protein tyrosine kinase-binding (TKB) domain, linker region, a RING (RING) finger (RF) domain, a proline-rich region, and a ubiquitin-associated region (Liu et al., 2014; Tang et al., 2019). The RF domain recruits E2 ubiquitin-conjugating enzymes which add ubiquitin to target substrates. The TKB domain recognizes specific phosphotyrosine residues on substrates for ubiquitin conjugation (Liu et al., 2014; Tang et al., 2019; Zhang, 2004). Previously, we and others have shown that Cbl-b is involved as a gatekeeper in the maintenance of a balance between immunity and tolerance (Bachmaier et al., 2000; Chiang et al., 2000; Heissmeyer et al., 2004; Jeon et al., 2004; Li et al., 2004; Zhang et al., 2002).

Genome-wide association studies (GWAS) have linked *CBLB* gene polymorphisms with patients with multiple sclerosis (MS) (Corrado et al., 2011; Sanna et al., 2010). *CBLB* polymorphisms can be associated with abnormalities in T cell function and responses to interferon-β therapy (Sturner et al., 2014). It was proposed that *CBLB* polymorphisms may affect the expression of *CBL-B* in T cells, thus mediating the disease process (Sturner et al., 2014). In support of these findings, loss of Cbl-b in mice facilitates the development of experimental autoimmune encephalomyelitis (EAE) (Chiang et al., 2000; Gruber et al., 2009), a mouse model of MS, and collagen-induced arthritis (Jeon et al., 2004), a mouse model of rheumatoid arthritis (RA), which are believed to be mediated at least in part by a pathogenic Th17 response. (Li et al., 2019; McGeachy et al., 2019; Sarkar et al., 2010) However, we have previously demonstrated that Cbl-b does not regulate Th1 and Th17 cell differentiation, but inhibits pro-allergic Th2/Th9 responses and allergic airway inflammation by targeting Stat-6 for ubiquitination and proteasome-mediated degradation (Qiao et al., 2014). Therefore, how Cbl-b regulates Th17 cell differentiation and Th17-mediated autoimmunity is currently unknown.

In this study, we utilized adoptive transfer and cell type-specific *Cblb* knockout strains to define the role of Cbl-b in priming of pathogenic Th17 cells and Th17-mediated autoimmunity using EAE as a model. We found that mice deficient for Cbl-b in macrophages, but not T cells and dendritic cells (DCs), develop severe EAE and a heightened pathogenic Th17 response, and that this is possibly achieved by aberrant IL-6 production by macrophages via CARD9-dependent CLR pathways, which facilitates the generation of pathogenic IL-17-producing $CD4^+$ T cells.

[1]Department of Pathology, The University of Iowa Roy J. and Lucille A. Carver College of Medicine, Iowa City, IA 52242, USA

[2]Department of Microbial Infection and Immunity, The Ohio State University, Columbus, OH 43210, USA

[3]Department of Neurology, Xiangya Hospital, Central South University, Changsha, Hunan, P.R. China

[4]Department of Cardiology, Xiangya Hospital, Central South University, Changsha, Hunan, P.R. China

[5]Department of Nephrology, Xiangya Hospital, Central South University, Changsha, Hunan, P.R. China

[6]Department of Neurology, The First Hospital of Changsha, Changsha, Hunan, P.R. China

[7]School of Biomedical Sciences, University of Western Australia, Perth, Australia

[8]Lead contact

*Correspondence: jian-zhang@uiowa.edu

https://doi.org/10.1016/j.isci.2022.105151

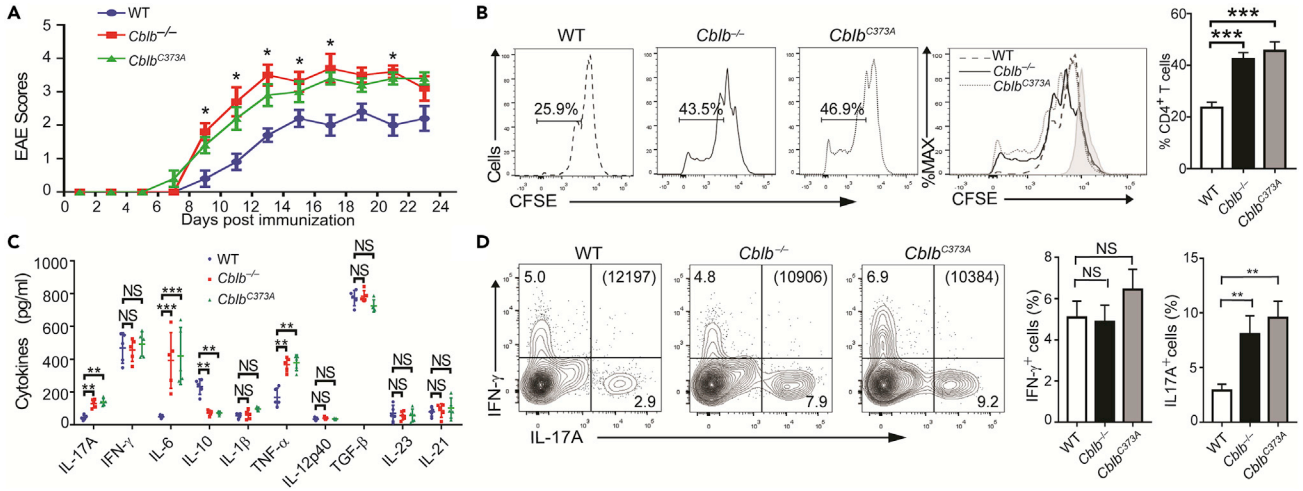

Figure 1. Loss or inactivation of Cbl-b in mice leads to the development of severe clinical symptoms of EAE

(A) Clinical scores of WT, *Cblb*$^{-/-}$, and *Cblb*^{C373A} mice (n = 5/group) immunized with MOG_{35-55} in CFA. *p < 0.05; Mann-Whitney U test.

(B and C) *Ex vivo* antigen-induced T cell proliferation and cytokine production of WT, *Cblb*$^{-/-}$, and *Cblb*^{C373A} mice (n = 3/group for B, n = 5/group for C) immunized with MOG_{35-55} in CFA as described in A, determined by CFSE labeling and ELISA. **p < 0.01, ***p < 0.001; Student t test.

(D) Flow cytometric analysis of Th1/Th17 responses in dLNs of WT, *Cblb*$^{-/-}$, and *Cblb*^{C373A} mice (n = 3/group) on day 8 after immunization with MOG_{35-55} in CFA. **p < 0.01; Student t test. Bracket: the total number of gated $CD4^+$ T cells. Data are one representative of three independent experiments.

RESULTS

Mice lacking Cbl-b or expressing an inactive form of Cbl-b develop severe EAE and display heightened Th17 responses

Several previous studies showed that *Cblb*$^{-/-}$ mice develop severe EAE (Chiang et al., 2000; Gruber et al., 2009) which is accompanied by a heightened Th17 response (Gruber et al., 2009). However, our previous study indicates that Cbl-b does not regulate Th17 but inhibits Th2/Th9 cell differentiation and Th2/Th9-mediated allergic airway inflammation (Qiao et al., 2014). To confirm whether Cbl-b inhibits EAE development and pathogenic Th17 responses via its E3 ubiquitin ligase activity, we immunized WT mice and mice lacking Cbl-b (Bachmaier et al., 2000) or expressing an E3 ubiquitin ligase dead mutation (C373A) (Oksvold et al., 2008) with myelin oligodendrocyte glycoprotein 35-55 peptide (MOG_{35-55}) in Complete Freund's Adjuvant (CFA) and monitored disease development for 23 days. In support of previous reports (Chiang et al., 2000; Gruber et al., 2009), mice with loss or inactivation of Cbl-b succumbed to severe disease (Figure 1A). This exacerbated disease was associated with hyper-proliferation of MOG_{35-55}-specific T cells, and heightened production of IL-17, TNF-α, and IL-6 in the supernatants of draining lymph node (dLN) cell cultures (Figures 1B and 1C). We did not see any significant changes in the production of IL-1β, IL12p40, and TGF-β, but IL-10 was significantly reduced in the culture of dLN cells lacking Cbl-b or expressing the Cbl-b C373A mutant (Figure 1C). To determine whether Cbl-b deficiency or inactivation potentiates an antigen-specific Th17 response, we immunized WT, *Cblb*$^{-/-}$, and *Cblb*^{C373A} mice with MOG_{35-55} in CFA, and Th1 and Th17 responses were monitored in the dLNs on day 8 after immunization. Loss or inactivation of Cbl-b in mice elicited a heightened Th17 response, while the Th1 response was comparable among WT, *Cblb*$^{-/-}$, and *Cblb*^{C373A} mice (Figure 1D). Our data strongly indicate that Cbl-b inhibits Th17 responses and Th17-mediated autoimmunity in an E3 ubiquitin ligase-dependent manner.

Cbl-b expression in macrophages but not T cells or DCs is responsible for exacerbated EAE and heightened pathogenic Th17 responses

To determine whether T cell intrinsic Cbl-b is required for the inhibition of EAE and Th17 responses *in vivo*, we first adoptively transferred $CD4^+$ T cells from WT and *Cblb*$^{-/-}$ mice into *Rag1*$^{-/-}$ recipients, which do not have T and B cells, and then immunized with MOG_{35-55} in CFA. Surprisingly, *Rag1*$^{-/-}$ mice receiving $CD4^+$ T cells from *Cblb*$^{-/-}$ mice developed EAE similar to those receiving WT $CD4^+$ T cells (Figure 2A). Further analysis showed that Th1 and Th17 cells in *Rag1*$^{-/-}$ mice receiving $CD4^+$ T cells from *Cblb*$^{-/-}$ mice were comparable to those receiving WT $CD4^+$ T cells (Figure 2B). To further confirm this, we generated mice with a *Cblb* allele mutated by insertion of two *loxP* sites flanking parts of the exon 5 (Tang et al., 2020). We crossed *Cblb*$^{f/f}$ mice with *Cd4 Cre* mice to generate *Cd4 Cre-Cblb*$^{f/f}$ mice to specifically delete

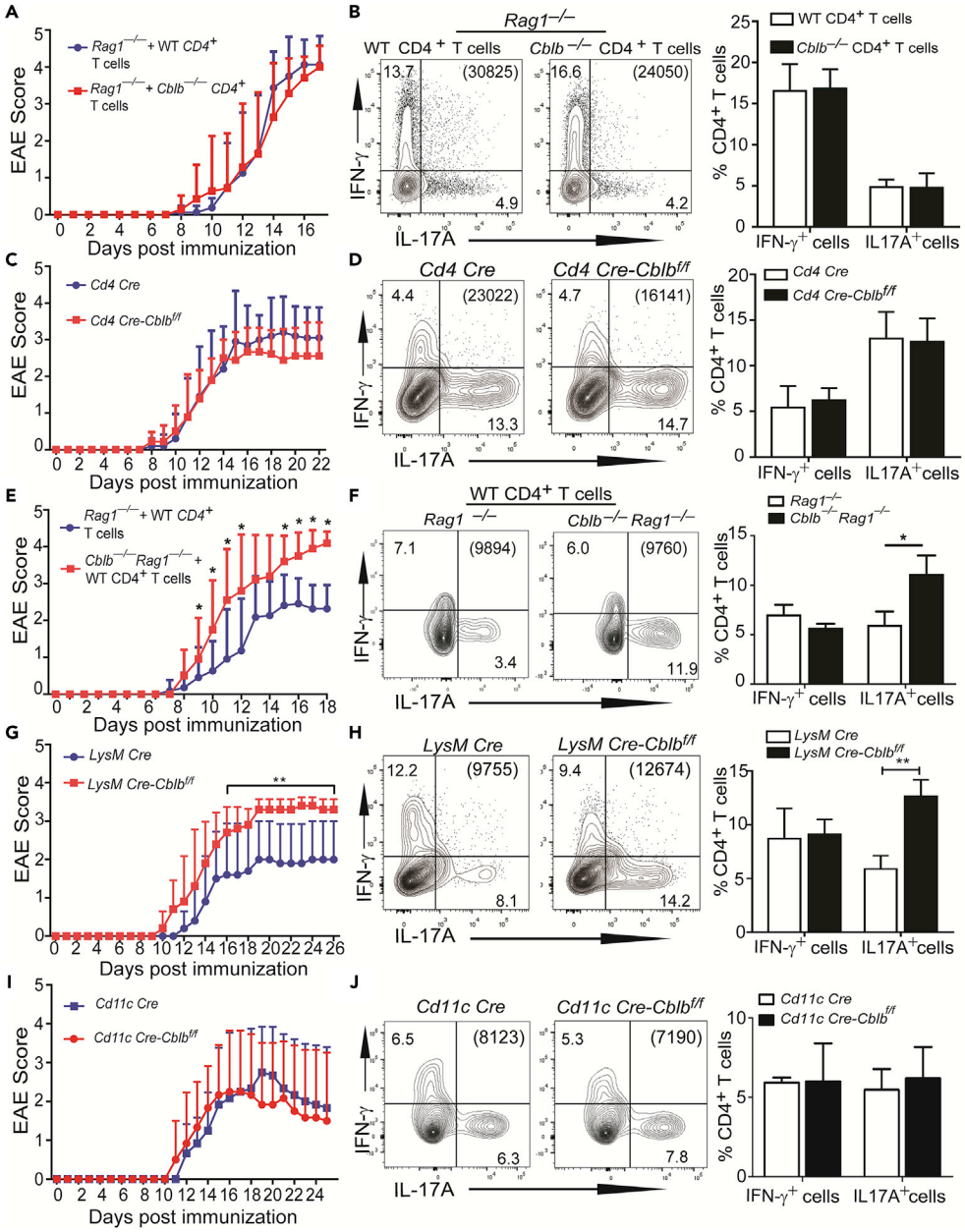

Figure 2. Cbl-b deficiency in myeloid cells is responsible for heightened EAE and Th17 responses

(A) Clinical scores of *Rag1*$^{-/-}$ mice receiving CD4$^+$ T cells from WT (n = 8) and *Cblb*$^{-/-}$ (n = 7) mice, immunized with MOG_{35-55} in CFA.

(B) Flow cytometric analysis of Th1/Th17 responses in dLNs of *Rag1*$^{-/-}$mice receiving CD4$^+$ T cells from WT and *Cblb*$^{-/-}$ mice (n = 3/group) on day 8 after immunization with MOG_{35-55} in CFA.

(C) Clinical scores of *Cd4 Cre* (n = 10) and *Cd4 Cre-Cblb*$^{f/f}$ (n = 9) mice, immunized with MOG_{35-55} in CFA.

(D) Flow cytometric analysis of Th1/Th17 responses in dLNs of *Cd4 Cre* and *Cd4 Cre-Cblb*$^{f/f}$ mice (n = 3/group) on day 8 after immunization with MOG_{35-55} in CFA.

(E) Clinical scores of *Rag1*$^{-/-}$ (n = 11) and *Cblb*$^{-/-}$*Rag1*$^{-/-}$ (n = 10) mice receiving CD4$^+$ T cells from WT mice, immunized with MOG_{35-55} in CFA. *p < 0.05; Mann-Whitney U test.

(F) Flow cytometric analysis of Th1/Th17 responses in dLNs of *Rag1*$^{-/-}$ and *Cblb*$^{-/-}$*Rag1*$^{-/-}$ mice (n = 4/group) receiving CD4$^+$ T cells from WT mice on day 8 after immunization with MOG_{35-55} in CFA. *p < 0.05; Student t test.

(G) Clinical scores of *LysM Cre* and *LysM Cre-Cblb*$^{f/f}$ mice (n = 8/group), immunized with MOG_{35-55} in CFA. **p < 0.01; Mann-Whitney U test.

Figure 2. *Continued*

(H) Flow cytometric analysis of Th1/Th17 responses in dLNs of *LysM Cre* and *LysM Cre-Cblb*$^{f/f}$ mice (n = 3/group) on day 8 after immunization with MOG_{35-55} in CFA. **p < 0.01; Student *t* test. (I) Clinical scores of *Cd11c Cre* and *Cd11c Cre-Cblb*$^{f/f}$ mice (n = 6/group), immunized with MOG_{35-55} in CFA.

(J) Flow cytometric analysis of Th1/Th17 responses in dLNs of *Cd11c Cre* and *Cd11c Cre-Cblb*$^{f/f}$ mice (n = 3/group) on day 8 after immunization with MOG_{35-55} in CFA. Bracket: the total number of gated $CD4^+$ T cells. Data are representative of two independent experiments.

Cbl-b in the T cell lineage (Figure S1A). We immunized *Cd4 Cre* and *Cd4 Cre-Cblb*$^{f/f}$ mice with MOG_{35-55} in CFA and monitored disease development. Consistent with the data in Figure 2A, the EAE scores in *Cd4 Cre* and *Cd4 Cre-Cblb*$^{f/f}$ mice were comparable (Figure 2C), which was associated with similar levels of Th1 and Th17 responses (Figure 2D). In support of this data, *ex vivo* cytokine production including IL-6, IL-17A, IFN-γ, TNF-α, IL-12p40, TGF-β, IL-1β, IL-23, and IL-21 in the supernatants of dLN cell cultures stimulated with MOG_{35-55} was comparable in *Cd4 Cre* and *Cd4 Cre-Cblb*$^{f/f}$ mice (Figure S2A). Therefore, our data collectively indicate that Cbl-b deficiency in T cells is not responsible for the exacerbated EAE and heightened Th17 response.

To test whether Cbl-b deficiency in innate immune cells may be responsible for the phenotype observed in *Cblb*$^{-/-}$ mice, we crossed *Cblb*$^{-/-}$ mice onto a *Rag1*$^{-/-}$ background to generate *Cblb*$^{-/-}$*Rag1*$^{-/-}$ mice which carry Cbl-b deficiency in innate immune cells. We adoptively transferred WT $CD4^+$ T cells into *Rag1*$^{-/-}$ and *Cblb*$^{-/-}$*Rag1*$^{-/-}$ mice and monitored the disease development for 18 days. As shown in Figure 2E, *Cblb*$^{-/-}$*Rag1*$^{-/-}$ mice receiving WT $CD4^+$ T cells developed severe EAE with an early onset. The severe disease was associated with an enhanced Th17 response (Figure 2F). To confirm this, we crossed *Cblb*$^{f/f}$ mice to *LysM Cre* and *Cd11c Cre* mice, respectively, to generate *LysM Cre-Cblb*$^{f/f}$ and *Cd11c Cre-Cblb*$^{f/f}$ mice which delete Cbl-b in myeloid cells, and DCs, respectively (Figures S1B and S1C). We immunized *LysM Cre* and *LysM Cre-Cblb*$^{f/f}$, or *Cd11c Cre*, and *Cd11c Cre-Cblb*$^{f/f}$ mice with MOG_{35-55} in CFA. Intriguingly, mice deficient for Cbl-b in myeloid cells (including monocytes, macrophages, and granulocytes), but not DCs, developed severe EAE with a significant increase in the Th17 response (Figures 2G–2J). This correlated with an increase in *ex vivo* cytokine production (IL-6, IL-17A, and TNF-α) by dLN cells from *LysM Cre-Cblb*$^{f/f}$ mice stimulated with MOG_{35-55} (Figure S2B). Note that TGF-β production was not increased in mice lacking Cbl-b in T cells (Figure S2A), suggesting that the increased Th17 response is not due to altered TGF-β signaling. Interestingly, IL-10 production was lower in dLN cell culture in the presence of MOG_{35-55} of *LysM Cre-Cblb*$^{f/f}$ than *LysM Cre* mice (Figure S2B). In addition, mice deficient for Cbl-b in myeloid cells had similar Treg cells compared with control mice (Figures S3A and S3B). These results indicate that the severe EAE observed in mice deficient for Cbl-b in myeloid cells is not due to defective Treg cells. Furthermore, there were no differences in the percentage and numbers of Tregs in mice sufficient or deficient for Cbl-b in T cells (Figure S2B).

IL-6 produced by *Cblb*$^{-/-}$ macrophages potentiates a pathogenic Th17 cell response

To define the cellular basis of this finding, we performed a co-culture experiment. We incubated $CD4^+$ T cells from 2D2 mice, which have transgenic expression of a MOG_{35-55}-specific TCR (Bettelli et al., 2003), together with bone-marrow-derived macrophages (BMDMs) or bone-marrow-derived dendritic cells (BMDCs) with MOG_{35-55} for 72 h in the presence of heat-killed *M.tb*. The cells were surface-stained with anti-CD4, and intracellularly stained with anti-IFN-γ and anti-IL-17. As shown in Figure 3A, 2D2 $CD4^+$ T cells co-cultured with *Cblb*$^{-/-}$ BMDMs, but not BMDCs, in the presence of heat-killed *M.tb*. skewed toward a Th17 phenotype compared to those co-cultured with WT BMDMs or BMDCs.

Macrophages can function both as antigen-presenting cells (APCs) and secrete pro-inflammatory cytokines such as IL-6, which can regulate a pathogenic Th17 cell response (Heink et al., 2017). To dissect these two functions of macrophages in Th17 cell differentiation, we pre-treated WT and *Cblb*$^{-/-}$ BMDMs with mitomycin C which inactivates macrophages but maintains their antigen presentation function. Pre-treating *Cblb*$^{-/-}$ macrophages with mitomycin C completely abrogated both $CD4^+$IFN-γ$^+$ and $CD4^+$IL-17$^+$ T cells in the presence of heat-killed *M.tb*. (Figure 3B), suggesting that the pro-inflammatory cytokines produced by *Cblb*$^{-/-}$ macrophages potentiate the Th17 cell response. Taken together, our data collectively indicate that the cytokines produced by *Cblb*$^{-/-}$ BMDMs strongly induced a pathogenic Th17 response.

IL-6 is a key cytokine to initiate Th17 cell differentiation (Heink et al., 2017; Korn et al., 2008). Several cellular sources including T cells, macrophages, and DCs can produce IL-6 (Couper et al., 2008; Heink et al., 2017). To

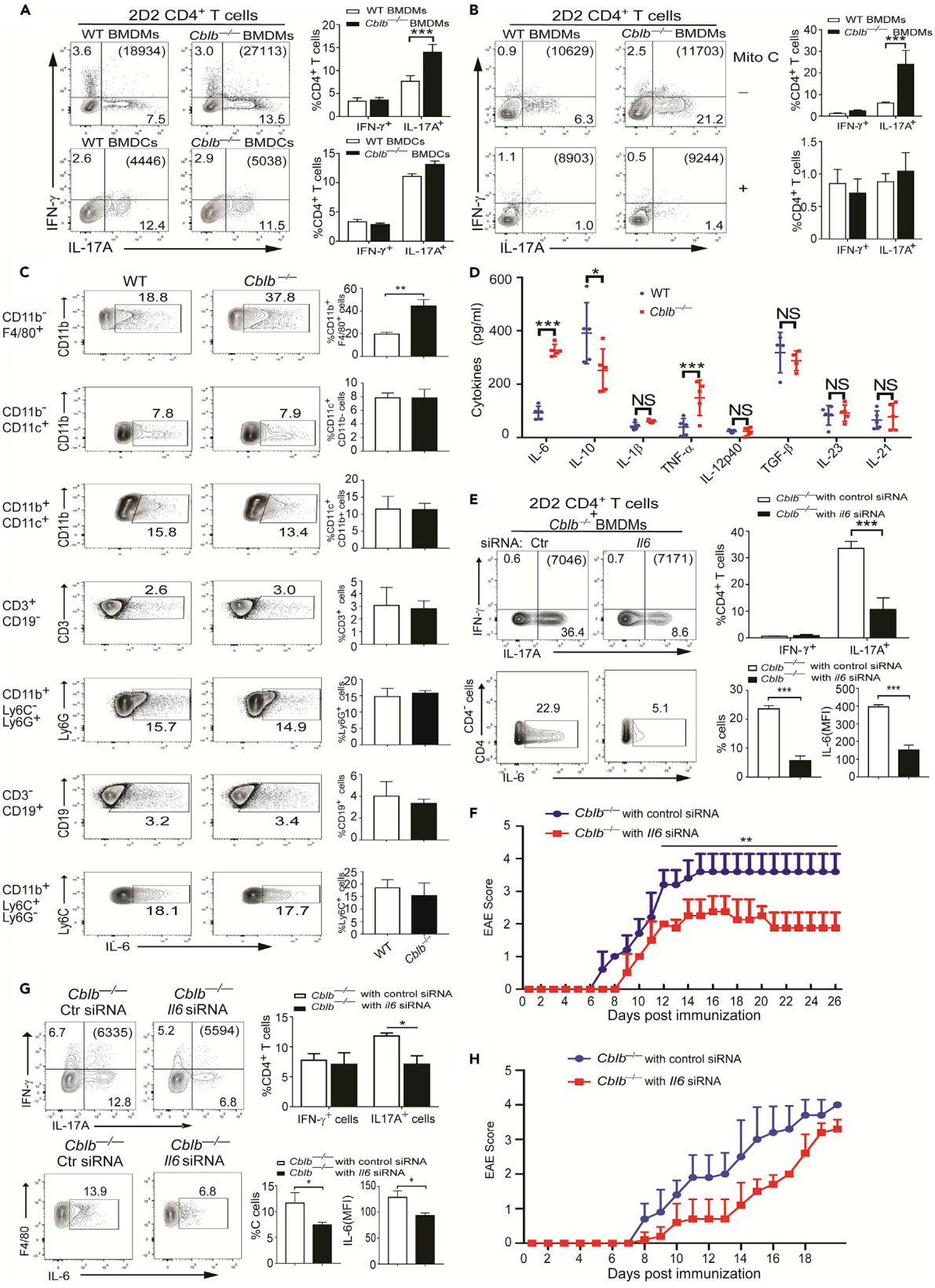
A
2D2 CD4+ T cells
WT BMDMs
Cblb−/− BMDMs
WT BMDCs
Cblb−/− BMDCs
IFN-γ
IL-17A
%CD4+ T cells
IFN-γ+
IL-17A+
B
2D2 CD4+ T cells
Mito C
C
WT
Cblb−/−
CD11b−
F4/80+
CD11b+
CD11c+
CD3+
CD19−
Ly6C−
Ly6G+
IL-6
D
Cytokines (pg/ml)
IL-6
IL-10
IL-1β
TNF-α
IL-12p40
TGF-β
IL-23
IL-21
NS
E
2D2 CD4+ T cells
Cblb−/− BMDMs
siRNA: Ctr
Il6
Cblb−/− with control siRNA
Cblb−/− with Il6 siRNA
%CD4+ T cells
CD4
% cells
IL-6(MFI)
F
Cblb−/− with control siRNA
Cblb−/− with Il6 siRNA
EAE Score
Days post immunization
G
Cblb−/−
Ctr siRNA
Il6 siRNA
F4/80
%C cells
IFN-γ+ cells
IL17A+ cells
H
Cblb−/− with control siRNA
Cblb−/− with Il6 siRNA
EAE Score
Days post immunization

Figure 3. Hyper-production of IL-6 by *Cblb*$^{-/-}$ macrophages promotes a pathogenic Th17 response

(A) Th1/Th17 cell differentiation in co-cultures of 2D2 T cells with BMDMs or BMDCs from WT and *Cblb*$^{-/-}$ mice (n = 3/group) in the presence of heat-killed *M.tb* and MOG_{35-55}. ***p < 0.001; Student *t* test.

(B) Th1/Th17 cell differentiation in co-cultures of 2D2 T cells with BMDMs from WT and *Cblb*$^{-/-}$ mice (n = 3/group) in the presence of heat-killed M.tb and MOG_{35-55} with or without pretreatment with mitomycin C. ***p < 0.001; Student *t* test.

(C) Flow cytometric analysis of IL-6-producing cells of dLNs of WT and *Cblb*$^{-/-}$ mice (n = 3/group) on day 8 after immunization with MOG_{35-55} in CFA, and stimulated with PMA/ionomycin. The gating strategy and representative plots see Figure S5. **p < 0.01; Student *t* test.

(D) ELISA of pro-inflammatory cytokines (TNF-α, IL-6, IL-10, IL-12p40, IL-1β, TGF-β, IL-23, and IL-21) by BMDMs from WT and *Cblb*$^{-/-}$ mice (n = 5/group) stimulated with heat-killed *M.tb*. *p < 0.05, ***p < 0.001; Student *t* test.

(E) Th1/Th17 cell differentiation in co-cultures of 2D2 $CD4^+$ T cells with BMDMs from *Cblb*$^{-/-}$ mice that had been treated with *Il6* or control siRNA. IL-6-producing macrophages of *Cblb*$^{-/-}$ mice treated with *Il6* (n = 4) or control siRNA (n = 4) were also determined. The mean fluorescent intensity (MFI) determined by flow cytometry indicates the expression level of IL-6 in $CD4^-$ macrophages of *Cblb*$^{-/-}$ mice treated with *Il6* or control siRNA. ***p < 0.001; Student *t* test.

(F) Clinical scores of *Cblb*$^{-/-}$ mice immunized with MOG_{35-55} in CFA in the treatment with or without *Il6* siRNA (n = 5) or control siRNA (n = 5) on day 1, 3, and 7 via tail vein injection. **p < 0.01; Mann-Whitney U test.

(G) Flow cytometric analysis of Th1/Th17 responses and IL-6-producing cells in dLN cells from *Cblb*$^{-/-}$ mice treated with *Il6* (n = 3) or control siRNA (n = 3) via tail vein injection as in F on day 8 after immunization with MOG_{35-55} in CFA. MFI determined by flow cytometry indicates the expression level of IL-6 in $F4/80^+$ cells from dLNs of *Cblb*$^{-/-}$ mice treated with *Il6* (n = 3) or control siRNA (n = 3). *p < 0.05; Student *t* test.

(H) Clinical scores of *Cblb*$^{-/-}$ mice immunized with MOG_{35-55} in CFA in the treatment with or without Il6 siRNA (n = 5) or control siRNA (n = 5) on day 8, 11, and 15 via tail vein injection. Bracket: the total number of gated $CD4^+$ T cells. Data are representative of three independent experiments (A, B, E, F, and G) and representative of two independent experiments (C-D).

further confirm whether Cbl-b deficiency in macrophages leads to heightened IL-6 production, we immunized WT and *Cblb*$^{-/-}$ mice with MOG_{35-55} in CFA. Eight days later we analyzed IL-6-producing macrophages ($CD11b^+F4/80^+$), DCs ($CD11b^-CD11c^+$ and $CD11b^+CD11c^+$), monocytes/neutrophils ($CD11b^+Ly6C^+Ly6G^-$/$CD11b^+Ly6C^-Ly6G^+$), $CD3^-CD19^+$ B cells, and $CD3^+CD4^+$ T cells in the dLNs. Interestingly, we observed that there were significantly more IL-6-producing macrophages from *Cblb*$^{-/-}$ mice than WT mice (Figure 3C). In contrast, there was no significant difference observed in IL-6-producing T cells, B cells, DCs, monocytes, or neutrophils from WT and *Cblb*$^{-/-}$ mice (Figure 3C), further confirming that IL-6 derived from macrophages lacking Cbl-b is the major source that mediates a pathogenic Th17 response during EAE induction. Consistent with this finding, BMDMs derived from *Cblb*$^{-/-}$ mice produced significantly more TNF-α and IL-6, and lesser amounts of IL-10, upon stimulation with heat-killed *M.tb*. in vitro (Figure 3D). The decreased IL-10 in *Cblb*$^{-/-}$ macrophages may be due to enhanced IL-6 production. Furthermore, we previously showed that there is no significant difference in TNF-α and IL-6 production by WT and *Cblb*$^{-/-}$ BMDMs upon LPS stimulation (Xiao et al., 2016). These findings are also consistent with our data presented Figure S2B in which IL-6 and TNF-α production was significantly increased in the supernatants collected from dLN cell culture from *LysM Cre-Cblb*$^{f/f}$ but not *Cd4 Cre-Cblb*$^{f/f}$ mice in an *ex vivo* MOG_{35-55} recall response.

To prove whether heightened IL-6 by *Cblb*$^{-/-}$ BMDMs facilitates a pathogenic Th17 response, we knocked down the *Il6* gene in *Cblb*$^{-/-}$ BMDMs by *Il6* siRNA, and then co-cultured 2D2 T cells with *Cblb*$^{-/-}$ BMDMs in the presence of MOG_{35-55} and heat-killed *M.tb* for 72 h. Silencing the *Il6* gene in *Cblb*$^{-/-}$ BMDMs markedly inhibited the Th17 cell response (Figure 3E). In further support of this data, treating *Cblb*$^{-/-}$ mice with *Il6* siRNA significantly ameliorated EAE disease activity (Figure 3F) and inhibited the Th17 response (Figure 3G). In addition, we treated siRNA during the onset stage (8 days after antigen immunization) and investigated the effect of *Il6* siRNA against EAE. In contrast to the data presented in Figure 3F, delayed treatment of *Cblb*$^{-/-}$ mice with *Il6* siRNA failed to suppress EAE progression (Figure 3H). Our data are consistent with a previous report that IL-6 blockade by an anti-IL-6 monoclonal antibody inhibits the induction of antigen-specific Th1 and Th17 cells in EAE (Serada et al., 2008).

CNS macrophages, but not neutrophils and microglia, from *Cblb*$^{-/-}$ mice with EAE produce more IL-6

To determine whether IL-6-producing macrophages in the CNS of *Cblb*$^{-/-}$ mice contribute to disease progression, and whether neutrophils or microglia also play a role in disease progression, we immunized WT and *Cblb*$^{-/-}$ mice with MOG_{35-55} in CFA, and 16–18 days later mice were sacrificed, and leukocytes from the spinal cords and brains were assessed for IL-6-producing cells in the CNS. As shown in Figure 4, IL-6-producing macrophages, but not neutrophils and microglia, were significantly enhanced in *Cblb*$^{-/-}$ mice compared to WT controls. These data further support a pathogenic role of IL-6 by macrophages in disease development.

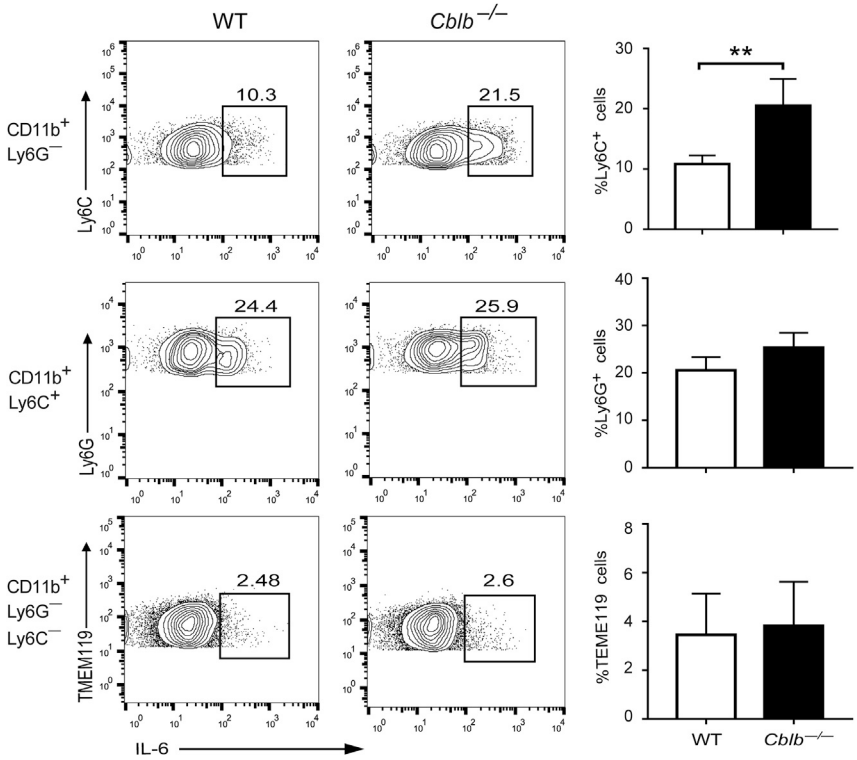

Figure 4. CNS macrophages, but not neutrophils and microglia, from *Cblb*$^{-/-}$ mice with EAE produce more IL-6

Flow cytometric analysis of IL-6-producing macrophages (CD11b^{+}Ly6C^{+}Ly6G), neutrophils(CD11b^{+}Ly6G^{+}Ly6C^{+}), and microglia (CD11b^{+}Ly6G^{-}Ly6C^{-}TMEM119^{+}) cells of CNS of WT and *Cblb*$^{-/-}$ mice (n = 4/group) on day 17 after immunization with MOG_{35-55} in CFA, and stimulated with PMA/ionomycin. **p < 0.01; Student *t* test. Data are representative of two independent experiments.

Deficiency for Dectin-2 but not Dectin-1 attenuates EAE disease activity in *Cblb*$^{-/-}$ mice

One major component in CFA is heat-killed *Mycobacterium tuberculosis* (*M.tb.*). *M.tb.* possess various cell wall components that influence host immune responses, such as trehalose-6,6′-dimycolate (TDM), mycolate, phosphatidyl-*myo*-inositol mannosides (PIMs), lipomannnan (LM), and lipoarabinomannan (LAM) (Wolfe et al., 2010). Dectin-2 is a direct receptor for mannose-capped LAM (Man-LAM) in *M.tb.* Mice lacking Dectin-2 (*Clec4n*) are resistant to EAE when heat-killed *M.tb.* is replaced with LAM (Yonekawa et al., 2014). Dectin-3 and Mincle recognize the *Mycobacterial* cord factor, TDM, and induce potent innate immune responses (Ishikawa et al., 2009; Matsunaga and Moody, 2009; Miyake et al., 2013; Zhao et al., 2014). Mice deficient for Dectin-3 (*Clec4d*) are resistant to EAE induction when using TDM as an adjuvant (Miyake et al., 2013). We previously showed that Dectin-2 and -3 are the targets for Cbl-b during fungal infections (Xiao et al., 2016). Since Dectins, in particular Dectin-2 and Dectin-3, have been shown to be required for the induction of EAE via their interactions with their ligands in *M.tb.*, a major component in CFA, we reasoned that the increased susceptibility to EAE and pathogenic Th17 response in *Cblb*$^{-/-}$ mice is due to aberrant expression of these Dectins, which correlates with our previous observation that Cbl-b targets Dectin receptors for ubiquitination and lysosome-mediated degradation (Xiao et al., 2016). Indeed, the expression of Dectin-2, -3, and Mincle was heightened in mice lacking Cbl-b (Figure S4).

To test this, we first determined whether loss of Dectin-2 attenuates the development of EAE in mice lacking Cbl-b, by generating *Cblb*$^{-/-}$*Clec4n*$^{-/-}$ mice. We also used *Clec7a*$^{-/-}$ and *Cblb*$^{-/-}$*Clec7a*$^{-/-}$ mice as controls, which are deficient for Dectin-1 or Dectin-1 and Cbl-b, respectively. In support of our prediction, loss of Dectin-2 attenuated the clinical scores in *Cblb*$^{-/-}$ mice to the levels of WT and *Clec4n*$^{-/-}$ mice (Figure 5A), which correlated with a decreased Th17 response (Figure 5B). Surprisingly, *Clec7a*$^{-/-}$ mice developed severe EAE and an enhanced Th17 response (Figures 5A and 5B), and Cbl-b deficiency did not worsen the disease in *Clec7a*$^{-/-}$ mice (Figures 5A and 5B). Given that we have shown that Cbl-b targets Dectin-1 for ubiquitination and lysosome-mediated degradation (Xiao et al., 2016), these data suggest that

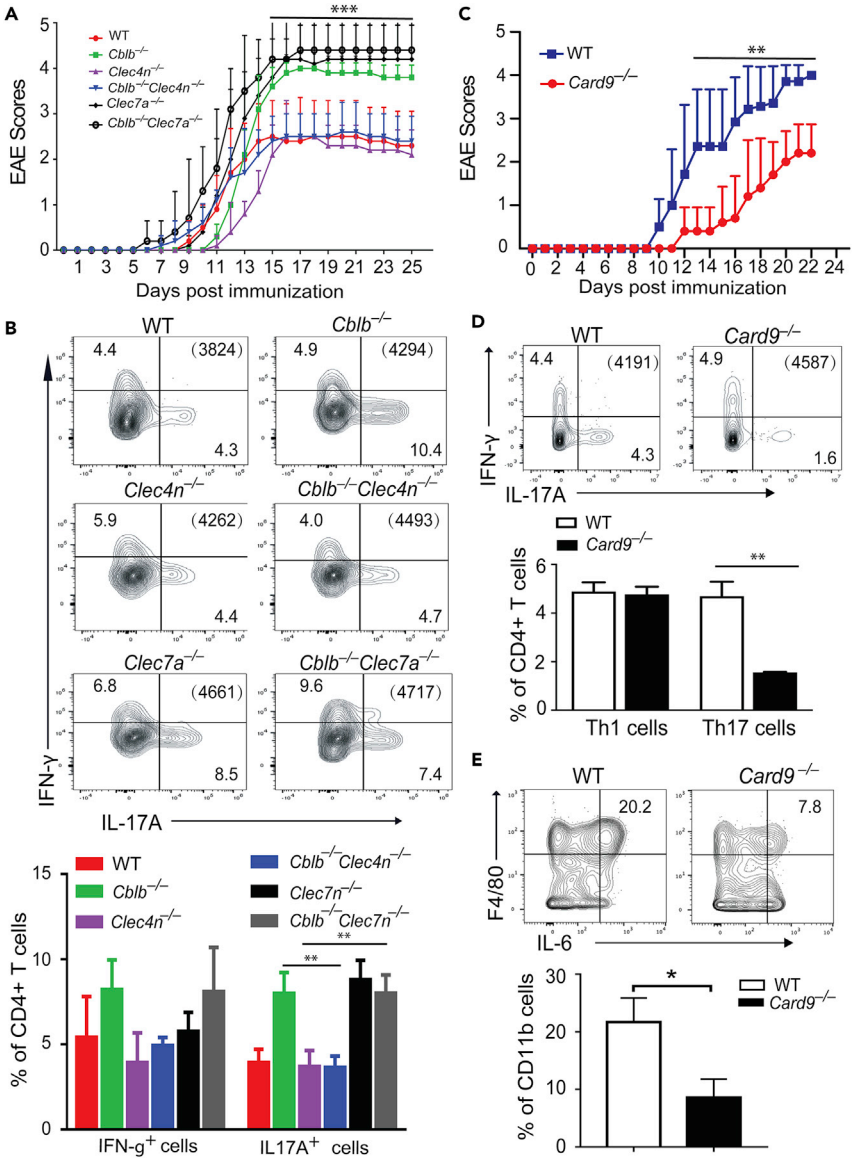

Figure 5. CARD9-mediated Dectin receptor signaling contributes the clinical symptoms of *Cblb*$^{-/-}$ mice with EAE and pathogenic Th17 response

(A) Clinical scores of WT, *Cblb*$^{-/-}$, *Clec4n*$^{-/-}$, *Clec7a*$^{-/-}$, *Cblb*$^{-/-}$*Clec4n*$^{-/-}$, and *Cblb*$^{-/-}$*Clec7a*$^{-/-}$ mice (n = 5/group) immunized with immunized with MOG_{35-55} in CFA. ***p < 0.001, Mann-Whitney U test.

(B) Flow cytometric analysis of Th1/Th17 responses in dLNs of WT, *Cblb*$^{-/-}$, *Clec4n*$^{-/-}$, *Clec7a*$^{-/-}$, *Cblb*$^{-/-}$*Clec7a*$^{-/-}$, and *Cblb*$^{-/-}$*Clec4n*$^{-/-}$ mice (n = 4/group) on day 8 after immunization with MOG_{35-55} in CFA. **p < 0.01, Student *t* test.

(C) Clinical scores of WT and *Card9*$^{-/-}$ mice (n = 7/group) immunized with MOG_{35-55} in CFA. **p < 0.01, Mann-Whitney U test.

(D) Flow cytometric analysis of Th1/Th17 responses in dLNs WT and *Card9*$^{-/-}$ mice (n = 5/group) on day 8 after immunization with MOG_{35-55} in CFA. **p < 0.01, Student's *t* test.

(E) Flow cytometric analysis of Th1/Th17 responses in dLNs WT and *Card9*$^{-/-}$ mice (n = 3/group) on day 8 after immunization with MOG_{35-55} in CFA. *p < 0.05, Student's *t* test. Data are three independent experiments for A and B, and two independent experiments for C, D, and E.

Cbl-b and Dectin-1 inhibit the development of EAE via different mechanisms. Although both Dectin-3 and Mincle are receptors for TDM, constitutive expression of Dectin-3 in myeloid cells is required for Mincle expression in response to TDM adjuvant (Miyake et al., 2013). Furthermore, TDM-induced EAE is almost completely dependent on Dectin-3, which is associated with a defective Th17 response (Miyake et al.,

2013). Therefore, it is possible that both Dectin-2 and Dectin-3/Mincle contribute to severe EAE in *Cblb*$^{-/-}$ mice. This notion is supported by the fact that congenic rats expressing lower levels of Dectin-3 and Mincle on myeloid cells exhibit a drastic reduction in EAE incidence and severity, which correlates with an impaired Th17 response in CNS (N'Diaye et al., 2020). Indeed, mice deficient for CARD9, the major adaptor protein which forms a complex with Bcl-10 and MALT-1 to induce the activation of NF-κB (Tang et al., 2018a), developed delayed and ameliorated EAE (Figure 5C), with a defective Th17 response (Figure 5D) and impaired macrophage-derived IL-6 (Figure 5E).

DISCUSSION

It has been well documented that mice deficient for Cbl-b develop severe EAE (Chiang et al., 2000; Gruber et al., 2009), and that *CBLB* polymorphisms are associated with MS disease activity (Corrado et al., 2011; Sanna et al., 2010; Sturner et al., 2014). However, the cellular and molecular mechanisms are poorly defined. In this study, we found that Cbl-b expression in myeloid cells, but not T cells, is responsible for restraining the priming of a pathogenic Th17 response, and this process is achieved by controlling the production of IL-6 by macrophages mediated by the signaling pathways of CARD9-dependent CLRs.

CBLB polymorphisms have been shown to associate with several autoimmune diseases in humans including MS, type 1 diabetes, and lupus (Bergholdt et al., 2005; Corrado et al., 2011; Doniz-Padilla et al., 2011; Sanna et al., 2010; Sturner et al., 2014). It was believed that Cbl-b deficiency leads to the impairment of T cell tolerance, thus resulting in aberrant autoreactive T cell proliferation (Bachmaier et al., 2000; Chiang et al., 2000; Jeon et al., 2004; Liu et al., 2014; Tang et al., 2018b). To our surprise, our previous data strongly indicate that Cbl-b does not inhibit Th17 cell differentiation, rather suppresses pro-allergic Th2/Th9 responses and allergic airway inflammation (Qiao et al., 2014). Our findings suggested that Cbl-b deficiency in innate immune cells may be responsible for heightened Th17 responses and severe EAE observed by other groups. Indeed, using *Rag1*$^{-/-}$ or *Cblb*$^{-/-}$*Rag1*$^{-/-}$ mice in combination with adoptive transfer, and conditional knockout strains specifically lacking Cbl-b in T cells, myeloid cells, and DCs, we demonstrate that loss of Cbl-b in macrophages leads to the aberrant production of pro-inflammatory cytokines which promote the differentiation of T cells into the pathogenic Th17 lineage and the development of EAE (Figure 2). This notion is supported by our recent study that *Cblb*$^{-/-}$ macrophages produce significantly more IL-6 and TNF-α upon infection with *Candida albicans* yeast and hyphal forms (Xiao et al., 2016).

IL-6 is a pleiotropic cytokine with significant functions in the regulation of the immune system. As a potent pro-inflammatory cytokine, IL-6 appears to play key roles in genetically diverse autoimmune diseases such as relapsing remitting MS, RA, and systemic lupus erythematosus (Choy et al., 2020; Kang et al., 2019). GWAS have confirmed that *CBLB* gene polymorphisms are associated with MS (Corrado et al., 2011; Sanna et al., 2010). It is possible that *CBLB* polymorphisms lead to increased IL-6 production by macrophages in patients with MS, which in turn leads to increased pathogenic Th17 cells and ultimately aggravates the disease. Indeed, macrophages, but not T cells, B cells, monocytes, DCs, or neutrophils from *Cblb*$^{-/-}$ mice during EAE induction produce more IL-6 than macrophages from WT mice (Figure 3C). By co-culturing 2D2 T cells with WT and *Cblb*$^{-/-}$ BMDMs or BMDCs, in the presence of heat-killed *M.tb*. and MOG_{35-55} peptide, we found that *Cblb*$^{-/-}$ BMDMs, but not BMDCs, facilitate 2D2 T cells to differentiate into Th17 cells which are abrogated when they are treated with mitomycin C (Figure 3B). This biased Th17 cell differentiation is most likely due to increased production of IL-6 by macrophages because 1) more IL-6 production was observed in *Cblb*$^{-/-}$ BMDMs stimulated with heat-killed *M.tb* (Figure 3D); 2) silencing the *Il6* gene in *Cblb*$^{-/-}$ BMDMs by *Il6* siRNA abrogates the heightened Th17 cell differentiation *in vitro* (Figure 3E); and 3) *in vivo* delivery of *Il6* siRNA inhibits the development of EAE in *Cblb*$^{-/-}$ mice (Figure 3F). Inhibition of IL-6 in *Cblb*$^{-/-}$ mice at the induction phase, but not after disease onset, suppresses disease progression (Figure S5), suggesting that targeting IL-6 to treat patients with active MS may not work. This notion is supported by the failure of anti-IL-6R treatment to suppress established EAE (Serada et al., 2008). A recent study reported that a Stat3 inhibitor ameliorates CNS autoimmunity in EAE by restoring the balance of Th17 vs. regulatory T cells (Tregs) (Aqel et al., 2021). IL-6, signaling through Stat3, induces the development of highly encephalitogenic Th17 cells (Das et al., 2009; Ghoreschi et al., 2010). IL-23, an inflammatory cytokine that is critical for EAE development and progression, signals through Stat3 and expands effector/memory myelin-specific Th17 cells in EAE mice (Ghoreschi et al., 2010; Langrish et al., 2005). Therefore, targeting signaling molecules downstream of IL-6/IL-23 such as Stat3 or IL-6 and IL-23 themselves may represent effective therapeutic strategies to treat MS via rebalancing pathogenic Th17:Tregs.

The development of MS involves both genetic and environmental factors such as viral infection. Several lines of evidence suggest that MS may be triggered by microbial infections. Indeed, fungi and bacteria have been directly identified in the CNS (Alonso et al., 2018). Indeed, *CBLB* variants have been shown to be associated with MS (Corrado et al., 2011; Sanna et al., 2010). *M.tb.* contain many TLR and CLR ligands (Faridgohar and Nikoueinejad, 2017; Miyake et al., 2013; Wassermann et al., 2015; Yonekawa et al., 2014) which can trigger inflammatory responses by innate immune cells. Since Dectin-2 deficiency fails to completely inhibit the development of EAE and Th17 responses in *Cblb*$^{-/-}$ mice (Figures 5A and 5B), it is possible that other CLRs such as Dectin-3 and Mincle may also be involved in the induction of the Th17 response. Indeed, mice deficient for Dectin-3 develop ameliorated EAE (Miyake et al., 2013), and congenic rats expressing lower levels of Dectin-3 and Mincle on myeloid cells exhibit a drastic reduction in EAE incidence and severity, which correlates with an impaired Th17 response in CNS (N'Diaye et al., 2020). Our data are further supported by the fact that *Card9*$^{-/-}$ mice develop significantly attenuated EAE and impaired pathogenic Th17 responses (Figures 5C and 5D). Our data are consistent with a recent report in which CARD9 has been shown to be required for the inflammatory pathology in experimental autoimmune uveoretinitis and Th17 responses (Lee et al., 2016). Note that our data indicate that *Card9*$^{-/-}$ mice still develop mild EAE (Figure 5C), suggesting that other signaling pathways may also be involved in EAE induction.

It was reported that Dectin-1 limits EAE and promotes myeloid cell-astrocyte crosstalk via a CARD9-independent expression of oncostatin M (Deerhake et al., 2021). However, the Th17 response was not altered in mice lacking Dectin-1 in this study (Deerhake et al., 2021) which is different from the data of our current study (Figures 5A and 5B). Nevertheless, our data, and those published by others (Deerhake et al., 2021), suggest that Dectin-1 may inhibit EAE development independently of CARD9. Therefore, the cellular and molecular mechanisms by which Dectin-1 inhibits EAE development are still not fully defined, and is currently under investigation in our laboratory.

In conclusion, we have provided compelling evidence that Cbl-b inhibits Th17 responses and Th17-mediated autoimmunity, and this inhibition is achieved by the suppression of IL-6 production by macrophages which directs T cells to differentiate into the Th17 cell lineage. Therefore, our study unveils a previously unsolved cellular mechanism how Cbl-b inhibits pathogenic Th17 responses.

Limitations of the study

Although GWAS studies have linked CBLB gene polymorphisms with patients with multiple sclerosis, it is still unknown whether CBLB gene polymorphisms lead to aberrant production of IL-6 by macrophages in patients with multiple sclerosis. In addition, how the interaction of Cbl-b-deficient macrophages with pathogenic Th17 cells plays a role in the pathogenesis of CNS demyelination needs to be explored in future studies.

STAR★METHODS

Detailed methods are provided in the online version of this paper and include the following:

- KEY RESOURCES TABLE
- RESOURCE AVAILABILITY
  - Lead contact
  - Materials availability
  - Data and code availability
- EXPERIMENTAL MODEL AND SUBJECT DETAILS
  - Mice
- METHOD DETAILS
  - EAE induction
  - $CD4^+$ isolation and *in vitro* $CD4^+$ T cells proliferation
  - Detection of Th1 and Th17 responses during EAE induction
  - $CD4^+$ T cells isolation and adoptive transfer for EAE induction
  - Generation of bone marrow-derived macrophages (BMDMs) and bone marrow-derived DCs (BMDCs)
  - Co-culture of 2D2 T cells with BMDMs or BMDCs
  - Treatment of BMDMs with mitomycin C
  - Determination of IL-6-producing cells by flow cytometry

SUPPLEMENTAL INFORMATION

Supplemental information can be found online at https://doi.org/10.1016/j.isci.2022.105151.

ACKNOWLEDGMENTS

We thank Drs. Josef M. Penninger, Gordon D. Brown and Yoichiro Iwakura for providing *Cblb*$^{-/-}$, *Clec7a*$^{-/-}$ and *Clec4n*$^{-/-}$ mice. This work was supported by the US National Institutes of Health (R01 AI090901, R01 AI121196, and R01 AI123253 to J.Z.). Q.Z. was supported by a Scholarship from the China Scholarship Council (CSC). J.Z. is a University of Iowa Health Care Distinguished Scholar.

AUTHOR CONTRIBUTIONS

Q.Z. and N.T. performed most *in vitro* and *in vivo* experiments, and analyzed the data; and Y.M., H.G., M.C.B., C.Y., R.T., Y.Z., and S.O. performed some *in vitro* and *in vivo* experiments; W.Y.L. and H.Y. helped with the design of the experiments, and edited the manuscript; J.Z. conceived and planned the research, and analyzed the data; and Q.Z., N.T., and J.Z. wrote the manuscript.

DECLARATION OF INTERESTS

The authors declare no competing financial interests.

INCLUSION AND DIVERSITY

We worked to ensure sex balance in the selection of non-human subjects.

We worked to ensure diversity in experimental samples through the selection of the cell lines.

While citing references scientifically relevant for this work, we also actively worked to promote gender balance in our reference list.

Received: November 9, 2020
Revised: August 6, 2022
Accepted: September 12, 2022
Published: October 21, 2022

REFERENCES

Alonso, R., Fernandez-Fernandez, A.M., Pisa, D., and Carrasco, L. (2018). Multiple sclerosis and mixed microbial infections. Direct identification of fungi and bacteria in nervous tissue. Neurobiol. Dis. *117*, 42–61.

Aqel, S.I., Yang, X., Kraus, E.E., Song, J., Farinas, M.F., Zhao, E.Y., Pei, W., Lovett-Racke, A.E., Racke, M.K., Li, C., and Yang, Y. (2021). A STAT3 inhibitor ameliorates CNS autoimmunity by restoring Teff:Treg balance. JCI Insight *6*.

Bachmaier, K., Krawczyk, C., Kozieradzki, I., Kong, Y.Y., Sasaki, T., Oliveira-dos-Santos, A., Mariathasan, S., Bouchard, D., Wakeham, A., Itie, A., et al. (2000). Negative regulation of lymphocyte activation and autoimmunity by the molecular adaptor Cbl-b. Nature *403*, 211–216.

Bergholdt, R., Taxvig, C., Eising, S., Nerup, J., and Pociot, F. (2005). CBLB variants in type 1 diabetes and their genetic interaction with CTLA4. J. Leukoc. Biol. *77*, 579–585.

Bettelli, E., Pagany, M., Weiner, H.L., Linington, C., Sobel, R.A., and Kuchroo, V.K. (2003). Myelin oligodendrocyte glycoprotein-specific T cell receptor transgenic mice develop spontaneous autoimmune optic neuritis. J. Exp. Med. *197*, 1073–1081.

Chiang, Y.J., Kole, H.K., Brown, K., Naramura, M., Fukuhara, S., Hu, R.J., Jang, I.K., Gutkind, J.S., Shevach, E., and Gu, H. (2000). Cbl-b regulates the CD28 dependence of T-cell activation. Nature *403*, 216–220.

Choy, E.H., De Benedetti, F., Takeuchi, T., Hashizume, M., John, M.R., and Kishimoto, T. (2020). Translating IL-6 biology into effective treatments. Nat. Rev. Rheumatol. *16*, 335–345.

Corrado, L., Bergamaschi, L., Barizzone, N., Fasano, M.E., Guerini, F.R., Salvetti, M., Galimberti, D., Benedetti, M.D., Leone, M., and D'Alfonso, S. (2011). Association of the CBLB gene with multiple sclerosis: new evidence from a replication study in an Italian population. J. Med. Genet. *48*, 210–211.

Couper, K.N., Blount, D.G., and Riley, E.M. (2008). IL-10: the master regulator of immunity to infection. J. Immunol. *180*, 5771–5777.

Das, J., Ren, G., Zhang, L., Roberts, A.I., Zhao, X., Bothwell, A.L., Van Kaer, L., Shi, Y., and Das, G. (2009). Transforming growth factor beta is dispensable for the molecular orchestration of Th17 cell differentiation. J. Exp. Med. *206*, 2407–2416.

Deerhake, M.E., Danzaki, K., Inoue, M., Cardakli, E.D., Nonaka, T., Aggarwal, N., Barclay, W.E., Ji, R.R., and Shinohara, M.L. (2021). Dectin-1 limits

autoimmune neuroinflammation and promotes myeloid cell-astrocyte crosstalk via Card9-independent expression of Oncostatin M. Immunity *54*, 484–498.e488.

Doniz-Padilla, L., Martinez-Jimenez, V., Nino-Moreno, P., Abud-Mendoza, C., Hernandez-Castro, B., Gonzalez-Amaro, R., Layseca-Espinosa, E., and Baranda-Candido, L. (2011). Expression and function of Cbl-b in T cells from patients with systemic lupus erythematosus, and detection of the 2126 A/G Cblb gene polymorphism in the Mexican mestizo population. Lupus *20*, 628–635.

Faridgohar, M., and Nikoueinejad, H. (2017). New findings of Toll-like receptors involved in Mycobacterium tuberculosis infection. Pathog. Glob. Health *111*, 256–264.

Ghoreschi, K., Laurence, A., Yang, X.P., Tato, C.M., McGeachy, M.J., Konkel, J.E., Ramos, H.L., Wei, L., Davidson, T.S., Bouladoux, N., et al. (2010). Generation of pathogenic T(H)17 cells in the absence of TGF-beta signalling. Nature *467*, 967–971.

Gruber, T., Hermann-Kleiter, N., Hinterleitner, R., Fresser, F., Schneider, R., Gastl, G., Penninger, J.M., and Baier, G. (2009). PKC-theta modulates the strength of T cell responses by targeting Cbl-b for ubiquitination and degradation. Sci. Signal. *2*, ra30.

Heink, S., Yogev, N., Garbers, C., Herwerth, M., Aly, L., Gasperi, C., Husterer, V., Croxford, A.L., Moller-Hackbarth, K., Bartsch, H.S., et al. (2017). Trans-presentation of IL-6 by dendritic cells is required for the priming of pathogenic TH17 cells. Nat. Immunol. *18*, 74–85.

Heissmeyer, V., Macian, F., Im, S.H., Varma, R., Feske, S., Venuprasad, K., Gu, H., Liu, Y.C., Dustin, M.L., and Rao, A. (2004). Calcineurin imposes T cell unresponsiveness through targeted proteolysis of signaling proteins. Nat. Immunol. *5*, 255–265.

Ishikawa, E., Ishikawa, T., Morita, Y.S., Toyonaga, K., Yamada, H., Takeuchi, O., Kinoshita, T., Akira, S., Yoshikai, Y., and Yamasaki, S. (2009). Direct recognition of the mycobacterial glycolipid, trehalose dimycolate, by C-type lectin Mincle. J. Exp. Med. *206*, 2879–2888.

Jeon, M.S., Atfield, A., Venuprasad, K., Krawczyk, C., Sarao, R., Elly, C., Yang, C., Arya, S., Bachmaier, K., Su, L., et al. (2004). Essential role of the E3 ubiquitin ligase Cbl-b in T cell anergy induction. Immunity *21*, 167–177.

Kang, S., Tanaka, T., Narazaki, M., and Kishimoto, T. (2019). Targeting Interleukin-6 signaling in clinic. Immunity *50*, 1007–1023.

Korn, T., Mitsdoerffer, M., Croxford, A.L., Awasthi, A., Dardalhon, V.A., Galileos, G., Vollmar, P., Stritesky, G.L., Kaplan, M.H., Waisman, A., et al. (2008). IL-6 controls Th17 immunity in vivo by inhibiting the conversion of conventional T cells into Foxp3+ regulatory T cells. Proc. Natl. Acad. Sci. USA *105*, 18460–18465.

Langrish, C.L., Chen, Y., Blumenschein, W.M., Mattson, J., Basham, B., Sedgwick, J.D., McClanahan, T., Kastelein, R.A., and Cua, D.J. (2005). IL-23 drives a pathogenic T cell population that induces autoimmune inflammation. J. Exp. Med. *201*, 233–240.

Lee, E.J., Brown, B.R., Vance, E.E., Snow, P.E., Silver, P.B., Heinrichs, D., Lin, X., Iwakura, Y., Wells, C.A., Caspi, R.R., and Rosenzweig, H.L. (2016). Mincle activation and the Syk/Card9 signaling Axis Are central to the development of autoimmune disease of the Eye. J. Immunol. *196*, 3148–3158.

Li, D., Gal, I., Vermes, C., Alegre, M.L., Chong, A.S., Chen, L., Shao, Q., Adarichev, V., Xu, X., Koreny, T., et al. (2004). Cutting edge: Cbl-b: one of the key molecules tuning CD28- and CTLA-4-mediated T cell costimulation. J. Immunol. *173*, 7135–7139.

Li, X., Bechara, R., Zhao, J., McGeachy, M.J., and Gaffen, S.L. (2019). IL-17 receptor-based signaling and implications for disease. Nat. Immunol. *20*, 1594–1602.

Liu, Q., Zhou, H., Langdon, W.Y., and Zhang, J. (2014). E3 ubiquitin ligase Cbl-b in innate and adaptive immunity. Cell Cycle *13*, 1875–1884.

Matsunaga, I., and Moody, D.B. (2009). Mincle is a long sought receptor for mycobacterial cord factor. J. Exp. Med. *206*, 2865–2868.

McGeachy, M.J., Cua, D.J., and Gaffen, S.L. (2019). The IL-17 family of cytokines in Health and disease. Immunity *50*, 892–906.

Miller, S.D., and Karpus, W.J. (2007). Experimental autoimmune encephalomyelitis in the mouse. Curr. Protoc. Immunol. *Chapter 15*. Unit 15 11.

Miyake, Y., Toyonaga, K., Mori, D., Kakuta, S., Hoshino, Y., Oyamada, A., Yamada, H., Ono, K., Suyama, M., Iwakura, Y., et al. (2013). C-type lectin MCL is an FcRgamma-coupled receptor that mediates the adjuvanticity of mycobacterial cord factor. Immunity *38*, 1050–1062.

N'Diaye, M., Brauner, S., Flytzani, S., Kular, L., Warnecke, A., Adzemovic, M.Z., Piket, E., Min, J.H., Edwards, W., Mela, F., et al. (2020). C-type lectin receptors Mcl and Mincle control development of multiple sclerosis-like neuroinflammation. J. Clin. Invest. *130*, 838–852.

Oksvold, M.P., Dagger, S.A., Thien, C.B., and Langdon, W.Y. (2008). The Cbl-b RING finger domain has a limited role in regulating inflammatory cytokine production by IgE-activated mast cells. Mol. Immunol. *45*, 925–936.

Ouyang, S., Zeng, Q., Tang, N., Guo, H., Tang, R., Yin, W., Wang, A., Tang, H., Zhou, J., Xie, H., et al. (2019). Akt-1 and Akt-2 Differentially regulate the development of experimental autoimmune encephalomyelitis by controlling proliferation of Thymus-derived regulatory T cells. J. Immunol. *202*, 1441–1452.

Qiao, G., Yang, L., Li, Z., Ying, H., Hassen, Y., Yin, F., and Zhang, J. (2012). Program death-1 regulates peripheral T cell tolerance via an anergy-independent mechanism. Clin. Immunol. *143*, 128–133.

Qiao, G., Ying, H., Zhao, Y., Liang, Y., Guo, H., Shen, H., Li, Z., Solway, J., Tao, E., Chiang, Y.J., et al. (2014). E3 Ubiquitin Ligase Cbl-b suppresses proallergic T cell development and allergic airway inflammation. Cell Rep. *6*, 709–723.

Rodriguez, C.I., Buchholz, F., Galloway, J., Sequerra, R., Kasper, J., Ayala, R., Stewart, A.F., and Dymecki, S.M. (2000). High-efficiency deleter mice show that FLPe is an alternative to Cre-loxP. Nat. Genet. *25*, 139–140.

Saijo, S., Ikeda, S., Yamabe, K., Kakuta, S., Ishigame, H., Akitsu, A., Fujikado, N., Kusaka, T., Kubo, S., Chung, S.H., et al. (2010). Dectin-2 recognition of alpha-mannans and induction of Th17 cell differentiation is essential for host defense against Candida albicans. Immunity *32*, 681–691.

Sanna, S., Pitzalis, M., Zoledziewska, M., Zara, I., Sidore, C., Murru, R., Whalen, M.B., Busonero, F., Maschio, A., Costa, G., et al. (2010). Variants within the immunoregulatory CBLB gene are associated with multiple sclerosis. Nat. Genet. *42*, 495–497.

Sarkar, S., Cooney, L.A., and Fox, D.A. (2010). The role of T helper type 17 cells in inflammatory arthritis. Clin. Exp. Immunol. *159*, 225–237.

Serada, S., Fujimoto, M., Mihara, M., Koike, N., Ohsugi, Y., Nomura, S., Yoshida, H., Nishikawa, T., Terabe, F., Ohkawara, T., et al. (2008). IL-6 blockade inhibits the induction of myelin antigen-specific Th17 cells and Th1 cells in experimental autoimmune encephalomyelitis. Proc. Natl. Acad. Sci. USA *105*, 9041–9046.

Sturner, K.H., Borgmeyer, U., Schulze, C., Pless, O., and Martin, R. (2014). A multiple sclerosis-associated variant of CBLB links genetic risk with type I IFN function. J. Immunol. *193*, 4439–4447.

Tang, J., Lin, G., Langdon, W.Y., Tao, L., and Zhang, J. (2018a). Regulation of C-type lectin receptor-mediated Antifungal immunity. Front. Immunol. *9*, 123.

Tang, J., Tu, S., Lin, G., Guo, H., Yan, C., Liu, Q., Huang, L., Tang, N., Xiao, Y., Pope, R.M., et al. (2020). Sequential ubiquitination of NLRP3 by RNF125 and Cbl-b limits inflammasome activation and endotoxemia. J. Exp. Med. *217*, e20182091.

Tang, R., Langdon, W.Y., and Zhang, J. (2018b). Regulation of Immune Responses by E3 Ubiquitin Ligase Cbl-B (Cell Immunol.).

Tang, R., Langdon, W.Y., and Zhang, J. (2019). Regulation of immune responses by E3 ubiquitin ligase Cbl-b. Cell. Immunol. *340*, 103878.

Wassermann, R., Gulen, M.F., Sala, C., Perin, S.G., Lou, Y., Rybniker, J., Schmid-Burgk, J.L., Schmidt, T., Hornung, V., Cole, S.T., and Ablasser, A. (2015). Mycobacterium tuberculosis Differentially Activates cGAS- and inflammasome-dependent intracellular immune responses through ESX-1. Cell Host Microbe *17*, 799–810.

Wolfe, L.M., Mahaffey, S.B., Kruh, N.A., and Dobos, K.M. (2010). Proteomic definition of the cell wall of Mycobacterium tuberculosis. J. Proteome Res. *9*, 5816–5826.

Xiao, Y., Qiao, G., Tang, J., Tang, R., Guo, H., Warwar, S., Langdon, W.Y., Tao, L., and Zhang, J. (2015). Protein tyrosine Phosphatase SHP-1 modulates T cell responses by controlling Cbl-b degradation. J. Immunol. *195*, 4218–4227.
Xiao, Y., Tang, J., Guo, H., Zhao, Y., Tang, R., Ouyang, S., Zeng, Q., Rappleye, C.A., Rajaram, M.V., Schlesinger, L.S., et al. (2016). Targeting

CBLB as a potential therapeutic approach for disseminated candidiasis. Nat. Med. *22*, 906–914.

Ying, H.Y., Yang, L.F., Qiao, G.L., Li, Z.P., Zhang, L., Yin, F., Xie, D., and Zhang, J.A. (2010). Cutting edge: CTLA-4-B7 interaction suppresses Th17 cell differentiation. J. Immunol. *185*, 1375–1378.

Yonekawa, A., Saijo, S., Hoshino, Y., Miyake, Y., Ishikawa, E., Suzukawa, M., Inoue, H., Tanaka, M., Yoneyama, M., Oh-Hora, M., et al. (2014). Dectin-2 is a direct receptor for mannose-capped lipoarabinomannan of mycobacteria. Immunity *41*, 402–413.

Zhang, J. (2004). Ubiquitin ligases in T cell activation and autoimmunity. Clin. Immunol. *111*, 234–240.

Zhang, J., Bardos, T., Li, D., Gal, I., Vermes, C., Xu, J., Mikecz, K., Finnegan, A., Lipkowitz, S., and Glant, T.T. (2002). Cutting edge: regulation of T cell activation threshold by CD28 costimulation through targeting Cbl-b for ubiquitination. J. Immunol. *169*, 2236–2240.

Zhao, X.Q., Zhu, L.L., Chang, Q., Jiang, C., You, Y., Luo, T., Jia, X.M., and Lin, X. (2014). C-Type lectin receptor Dectin-3 mediates trehalose 6,6′-dimycolate (TDM)-induced Mincle expression through CARD9/Bcl10/MALT1-dependent Nuclear factor (NF)-kappaB activation. J. Biol. Chem. *289*, 30052–30062.

STAR★METHODS

KEY RESOURCES TABLE

REAGENT or RESOURCE	SOURCE	IDENTIFIER
Antibodies		
anti-mouse CD28 (37.51)	BD Biosciences	Cat#: 553294; RRID:AB_394763
anti-CD3 (145-2C11)	BD Biosciences	Cat#: 550275; RRID:AB_393572
Mouse GM-CSF	R&D Systems	Cat#: 415-ML-010/CF
hamster IgG isotypic controls	BD Biosciences	Cat#: 553951; RRID:AB_395155
anti-mouse CD4-PerCP	BioLegend	Cat#: 100432; RRID:AB_893323
anti-mouse CD4-FITC	BioLegend	Cat#: 100406; RRID:AB_312691
anti-mouse CD4-allophycocyanin/Cy7	BioLegend	Cat#: 100414; RRID:AB_312699
anti-mouse CD3-allophycocyanin	BioLegend	Cat#: 100236; RRID:AB_2561456
anti-mouse CD11b-allophycocyanin	BioLegend	Cat#: 101212; RRID:AB_312795
anti-mouse CD11c-FITC	BioLegend	Cat#: 117306; RRID:AB_313775
anti-mouse F4/80-PE/Cy7	BioLegend	Cat#: 123114; RRID:AB_893478
anti-mouse Ly6G-Brilliant Violet 421	BioLegend	Cat#: 127628; RRID:AB_2562567
anti-mouse Foxp3-PE	BioLegend	Cat#: 320008; RRID:AB_492980
anti-mouse CD25-allophycocyanin	BioLegend	Cat#: 101910; RRID:AB_2280288
anti-mouse IL-17A-PE	BioLegend	Cat#: 506904; RRID:AB_315464
anti-mouse IFN-γ-allophycocyanin	BioLegend	Cat#: 505810; RRID:AB_315404
anti-mouse IL-6-FITC	eBioscience	Cat#: 11-7061-41; RRID:AB_1633408
anti-mouse CD19-Brilliant Violet 786	BD Biosciences	Cat#: 563333; RRID:AB_2738141
anti-mouse Ly6C-PerCP/Cy5.5	BD Biosciences	Cat#: 560525; RRID:AB_1727558
anti-mouse CD3-PE/Cy5	BioLegend	Cat#: 100273; RRID:AB_2894410
anti-mouse F4/80-PerCP/Cy5.5	BioLegend	Cat#: 157318; RRID:AB_2894410
anti-mouse CD11b-Pacific Blue	BioLegend	Cat#: 101224; RRID:AB_755986
anti-mouse TMEM119-PE/Cy7	ThermoFisher	Cat#: 25-6119-82; RRID:AB_2848312
anti-mouse IL-6-APC	BioLegend	Cat#: 504508; RRID:AB_10694868
anti-mouse CD45.2-Brilliant Violet 711	BioLegend	Cat#: 109847; RRID:AB_2616859
anti-mouse CD11b-Brilliant Violet 605	BioLegend	Cat#: 101257; RRID:AB_2565431
anti-mouse Ly-6C-PE	BioLegend	Cat#: 128008; RRID:AB_1186132
anti-mouse Ly-6G-FITC	BioLegend	Cat#: 127606; RRID:AB_1236494
anti-mouse Dectin-2-FITC	Miltenyi Biotec	Cat#: 130-125-214; RRID:AB_2889657
anti-mouse Dectin-1-PE	BioLegend	Cat#: 144304; RRID:AB_2561501
anti-mouse Dectin-3-APC	BioLegend	Cat#: 360206; RRID:AB_2563154
anti-mouse B220-PE/Cy7	BioLegend	Cat#: 103222; RRID:AB_313005
anti-mouse Cbl-b (H-121)	Santa Cruz	Cat#: sc-1704; RRID:AB_2070711
Chemicals, peptides, and recombinant proteins		
Mycobacterium tuberculosis strain H37Ra	Difco	Cat#: 231141
carboxyfluorescein succinimidyl ester (CFSE)	BioLegend	Cat#: 422701
Pertussis toxin	List Biological Laboratories	Cat#: 181
Myelin oligodendrocyte glycoprotein peptide 35–55	GL Biochem	NA
Incomplete Freund's Adjuvant (IFA)	Sigma-Aldrich	Cat#: F5506
Complete Freund's Adjuvant (CFA)	Sigma-Aldrich	Cat#: F5881

(*Continued on next page*)

Continued

REAGENT or RESOURCE	SOURCE	IDENTIFIER
Mitomycin C	Sigma-Aldrich	Cat#: 50-07-7
Ionomycin	Sigma-Aldrich	Cat#: I0634
Fixation/Permeabilization Concentrate	eBioscience	Cat#: 00-5123-43
Permeabilization Buffer (10X)	eBioscience	Cat#: 00-8333-56
PMA	Sigma-Aldrich	Cat#: 16561-29-8
Cytofix/Cytoperm solution	BD Bioscience	Cat#: 554714
Critical commercial assays		
$CD4^+$ T Cell Isolation Kits	Miltenyi Biotec	Cat#: 130-104-454
Pan Dendritic Cell Isolation Kit	Miltenyi Biotec	Cat#: 130-100-875
Mouse IL-17A ELISA MAX™ Deluxe Sets	BioLegend	Cat#: 432504
Mouse IL-10 ELISA MAX™ Deluxe Sets	BioLegend	Cat#: 431414
Mouse IFN-g ELISA MAX™ Deluxe Sets	BioLegend	Cat#: 430804
Mouse IL-1b ELISA MAX™ Deluxe Sets	BioLegend	Cat#: 432604
Mouse TNF-a ELISA MAX™ Deluxe Sets	BioLegend	Cat#: 430904
Mouse TGF-b ELISA LEGEND MAX™	BioLegend	Cat#: 433007
Mouse IL-23 ELISA MAX™ Deluxe Sets	BioLegend	Cat#: 433704
Mouse IL-21 ELISA LEGEND MAX™	BioLegend	Cat#: 446107
Mouse IL-6 ELISA MAX™ Deluxe Sets	BioLegend	Cat#: 431315
Experimental models: Organisms/strains		
Cblb$^{/}$ *mice*	Dr. Josef M. Penninger	N/A
2D2 TCR mice	Jackson Laboratory	RRID: IMSR_JAX:006912
Card9$^{-/-}$ mice	Jackson Laboratory	RRID: IMSR_JAX:028652
Clec7a$^{-/-}$ mice	Jackson Laboratory	RRID: IMSR_JAX:012337
LysM Cre mice	Jackson Laboratory	RRID: IMSR_JAX:004781
Cd4 Cre mice	Jackson Laboratory	RRID: IMSR_JAX:017336
Rag1$^{-/-}$ mice	Jackson Laboratory	RRID: IMSR_JAX:002216
Cd11c Cre mice	Jackson Laboratory	RRID: IMSR_JAX:008068
Cblb^{C373A} mice	(Oksvold et al., 2008)	N/A
Clec4n$^{-/-}$ mice	Dr. Yoichiro Iwakura	N/A
Cblb$^{-/-}$*Rag1*$^{-/-}$ mice	Mice crossed in our facility	N/A
Cblb$^{-/-}$*Clec4n*$^{-/-}$ mice	Mice crossed in our facility	N/A
Cblb$^{-/-}$*Clec7a*$^{-/-}$ mice	Mice crossed in our facility	N/A
Cblb$^{f/f}$ mice	Generated in-house	N/A
Cd4 Cre-Cblb$^{f/f}$mice	Mice crossed in our facility	N/A
LysM Cre-Cblb$^{f/f}$ mice	Mice crossed in our facility	N/A
Cd11c Cre-Cblb$^{f/f}$ mice	Mice crossed in our facility	N/A
Oligonucleotides		
Primer RNA:5′-CCCGGGCAAGGCTC AGCCATGCTCCTG-3′	Integrated DNA Technologies	N/A
Primer RNA:5′-GCGGCCGCAATTCC CAGAGACATCCCTCC-3′	Integrated DNA Technologies	N/A
Primer RNA:5′-CTAGGCCACAGAATT GAAAGATCT-3′	Integrated DNA Technologies	N/A
Primer RNA:5′-GTAGGTGGAAATTCTA GCATCATCC-3′	Integrated DNA Technologies	N/A

(*Continued on next page*)

Continued

REAGENT or RESOURCE	SOURCE	IDENTIFIER
Primer RNA:5′-CTGACAGGGAACA GAAGGTG-3′	Integrated DNA Technologies	N/A
Primer RNA:5′-TGCCTGCTTGCC GAATATC-3′	Integrated DNA Technologies	N/A
Primer RNA:5′-AGGACTTTGCAC TGGCGTAG-3′	Integrated DNA Technologies	N/A
Primer RNA:5′-GCCAATGCTGCC GACTCCAG-3′	Integrated DNA Technologies	N/A
Primer RNA:5′-GCTGTAACTTCT GAAGAAAAC-3′	Integrated DNA Technologies	N/A
Primer RNA:5′-GCGCGCCCCTCGA GCTAGAG-3′	Integrated DNA Technologies	N/A
Primer RNA:5′-TCTGGACTTGCCT CCTCTGT-3′	Integrated DNA Technologies	N/A
Primer RNA:5′-CATTCCATCGCAAG ACTCCT-3′	Integrated DNA Technologies	N/A
Primer RNA:5′-TGGATGTGGAA TGTGTGCGAG-3′	Integrated DNA Technologies	N/A
Primer RNA:5′-AAGGAGGGAC TTGGAGGATG-3′	Integrated DNA Technologies	N/A
Primer RNA:5′-GTCACTCACTGCTC CCCTGT-3′	Integrated DNA Technologies	N/A
Primer RNA:5′-ACCGGTAATGCAG GCAAAT-3′	Integrated DNA Technologies	N/A
Primer RNA:5′-GCGGTCTGGCAGTA AAAACTATC-3′	Integrated DNA Technologies	N/A
Primer RNA:5′-GTGAAACAGCATTG CTGTCACTT-3′	Integrated DNA Technologies	N/A
Primer RNA:5′-CTAGGCCACAGAAT TGAAAGATCT-3′	Integrated DNA Technologies	N/A
Primer RNA:5′-GTAGGTGGAAATTC TAGCATCATCC-3′	Integrated DNA Technologies	N/A
Primer RNA:5′-ACTTGGCAGCTGT CTCCAAG-3′	Integrated DNA Technologies	N/A
Primer RNA:5′-GCGAACATCTTCA GGTTCTG-3′	Integrated DNA Technologies	N/A
Primer RNA:5′-CAAATGTTGCTT GTCTGGTG-3′	Integrated DNA Technologies	N/A
Primer RNA:5′-GTCAGTCGAG TGCACAGTTT-3′	Integrated DNA Technologies	N/A
Recombinant DNA		
Accell Il6 siRNA	Dharmanon	Cat#: L-043739-00-0005
non-sense siRNA	Horizon Discovery	Cat#: D-001206-14-05
Software and algorithms		
FlowJo	FlowJo, LLC and Illumina, Inc	https://www.flowjo.com/
GraphPad Prism 7.0	GraphPad Software, Inc.	https://www.graphpad.com/
SPSS software	IBM	https://www.ibm.com/analytics/spss-statistics-software

(*Continued on next page*)

Continued

REAGENT or RESOURCE	SOURCE	IDENTIFIER
Image Lab Software	Bio-Red	https://www.bio-rad.com/
Adobe illustrator	Adobe	https://www.adobe.com/products/illustrator.html#

RESOURCE AVAILABILITY

Lead contact

Further information and requests for resources and reagents should be directed to and will be fulfilled by the lead contact, Jian Zhang (jian-zhang@uiowa.edu).

Materials availability

Requests for further information or materials should be directed to the lead contact.

Data and code availability

- Data reported in this paper will be shared by the lead contact upon request.
- Requests for biological datasets should be directed to the lead contact.
- This paper does not report original code. Any additional information required to reanalyze the data reported in this paper is available from the lead contact upon request.

EXPERIMENTAL MODEL AND SUBJECT DETAILS

Mice

C57BL/6, 2D2 TCR transgenic, *Card9*$^{-/-}$, *Clec7a*$^{-/-}$, *Cd4 Cre*, *LysM Cre*, *Cd11c Cre*, and B6.129S7-*Rag1*$^{tm1Mom/J}$ (*Rag1*$^{-/-}$) mice were purchased from The Jackson Laboratory (Bar Harbor, ME). *Cblb*$^{-/-}$ mice were kindly provided by Dr. Josef M. Penninger (University of Toronto; Toronto, ON, Canada). *Cblb*^{C373A} mice were described previously (Oksvold et al., 2008). *Clec4n*$^{-/-}$ mice (Saijo et al., 2010) were obtained from Dr. Yoichiro Iwakura (Tokyo University of Science; Chiba, Japan). *Cblb*$^{-/-}$ mice were crossed with *Rag1*$^{-/-}$, *Clec4n*$^{-/-}$, and *Clec7a*$^{-/-}$ mice to generate *Cblb*$^{-/-}$*Rag1*$^{-/-}$, *Cblb*$^{-/-}$*Clec4n*$^{-/-}$, and *Cblb*$^{-/-}$*Clec7a*$^{-/-}$ mice.

The mouse strain carrying the *Cblb*$^{tm1a(KOMP)Wtsi}$ allele was generated at the Ohio State University Genetically Engineered Mouse Modeling Core Facility by standard embryonic stem (ES) cell technology as described previously (Tang et al., 2020). The ES clone EPD0703_2_B11 was acquired from the International Knockout Mouse Phenotyping Consortium (IMPC project #79117). Prior to microinjection, the identity of the targeted embryonic stem cells was verified by 5′ long-range PCR using a primer external to the targeting vector. Chimeric males were bred to C57BL/6 Albino females and germline transmission was verified by PCR to detect the mutant together with the wild-type allele in the F1 heterozygous mice. Prior to utilization of the strain for experiments, mice were crossed to a Flipe ubiquitous strain (ACTB:FLPe B6J, JAX strain # 005703) (Rodriguez et al., 2000) to eliminate the lacZ/neo cassette and obtain the clean tm1c allele according to the breeding schemes recommended by the IMPC. The LoxP flanked *Cblb* allele (*Cblb*$^{f/f}$) was crossed to *Cd4 Cre*, *LysM Cre*, and *Cd11c Cre* mice to specifically delete Cbl-b in T cells, myeloid cells including macrophages, and DCs. All mice were bred and housed under specific pathogen–free (SPF) conditions. The experimental protocols followed National Institutes of Health guidelines and were approved by the Institutional Animal Care and Use Committees of The Ohio State University and the University of Iowa. All mice were used for experiments at ages of 8–12 weeks, and both male and female mice were used in this study.

METHOD DETAILS

EAE induction

Various groups of mice at 8-12 weeks were subcutaneously (s.c.) injected over four sites in the flank with 100 μL of emulsified IFA supplemented with 200 μg of $MOG_{33–55}$ and 500 μg of heat-killed *M.tb* as previously described (Ouyang et al., 2019; Xiao et al., 2015). Three hundred ng pertussis toxin (List) per mouse in PBS was injected intraperitoneally (i.p.) at the time of immunization and 48 h later. The mice were

monitored daily for clinical signs of EAE, and were scored on a scale of 0–5 (Miller & Karpus, 2007): 0, no clinical disease; 1, limp/flaccid tail; 2, moderate hindlimb weakness; 3, severe hindlimb weakness; 4, complete hindlimb paralysis; and 5, quadriplegia or premoribund state.

$CD4^+$ isolation and *in vitro* $CD4^+$ T cells proliferation

$CD4^+$ T cells from WT, *Cblb*$^{-/-}$ and *Cblb*^{C373A} mice immunized with MOG_{35-55} in CFA were isolated by the $CD4^+$ T cell Isolation Kit (Miltenyi Biotec). The $CD4^+$ T cells were labeled with CFSE and cultured with 20 μg/mL MOG_{35-55} in the presence of irradiated splenocytes depleted of T cells for 72 h. The proliferation rates of $CD4^+$ T cells were determined by CFSE dilution. The supernatants collected from these cultures were subjected for ELISA for IL-17A, IFN-γ, IL-12p40, IL-6, IL-10, IL-1β, TNF-α, TGF-β, IL-21 and IL-23 using sandwich ELISA kits (BioLegend). All the procedures were performed according to the manufacturer's instructions.

Detection of Th1 and Th17 responses during EAE induction

For detection of Th1 and Th17 responses, dLN cells collected from various groups of mice immunized with MOG_{35-55} in CFA on day 8 were stimulated with 20 μg/mL MOG_{35-55} in culture medium for 3 days. The supernatants collected from these cultures were subjected for ELISA for IL-17A, IFN-γ, IL-12p40, IL-6, IL-10, IL-1β, TNF-α, TGF-β, IL-21 and IL-23 using the sandwich ELISA kits (BioLegend). The cells were restimulated with 50 ng/mL PMA and 750 ng/mL ionomycin for 4 h. The cells were surface-stained with anti-CD4, and intracellularly stained with anti-IFN-γ or anti-IL-17, respectively. The $CD4^+$IFN-γ^+ and $CD4^+$IL-17^+ cells were determined by flow cytometry as previously described (Qiao et al., 2012, 2014; Xiao et al., 2015; Ying et al., 2010).

$CD4^+$ T cells isolation and adoptive transfer for EAE induction

$CD4^+$ T cells from WT and *Cblb*$^{-/-}$ mice were isolated by the $CD4^+$ T cell Isolation Kit (Miltenyi Biotec) and injected into *Rag1*$^{-/-}$ mice by i.v. at 5×10^6 cells/mouse. In a separate experimental setting, $CD4^+$ T cells from WT mice were adoptively transferred into *Rag1*$^{-/-}$ and *Rag1*$^{-/-}$*Cblb*$^{-/-}$ mice, respectively. Thirty days later, the recipient mice were immunized with MOG_{35-55} in CFA.

Generation of bone marrow-derived macrophages (BMDMs) and bone marrow-derived DCs (BMDCs)

Erythrocyte-depleted mouse bone marrow (BM) cells were cultured from WT and *Cblb*$^{-/-}$ mice strains and were harvested from the femurs and tibias of mice. Cells were cultured in DMEM containing 10% FBS and 30% conditioned medium from L929 cells expressing M-CSF as described (Xiao et al., 2016). After one week of culture, non-adherent cells were removed, and adherent cells were 80-90% F4/80$^+$CD11b$^+$ as determined by flow cytometric analysis.

For BMDC generation, bone marrow cells were cultured in RPMI supplemented with 10% fetal calf serum, 2 mM L-glutamine, 100 U/ml penicillin, 0.1 mg/mL streptomycin, 0.05 mM β-mercaptoethanol and 20 ng/mL GM-CSF (R&D Systems, Minneapolis, MN). The cultures were usually fed every 2 days by gently swirling the plates, aspirating 75% of the medium, and adding back fresh medium with GM-CSF. After 7-8 days, DMDCs were enriched by a DC enrichment kit (Miltenyi Biotec).

Co-culture of 2D2 T cells with BMDMs or BMDCs

$CD4^+$ T cells from 2D2 mice were incubated with BMDMs or BMDCs pre-pulsed with 20 μg/mL of MOG_{35-55} peptide overnight in the presence of 20 μg/mL of heat-killed *M.tb* at a 1:1 ratio. On day 3, the cells were stimulated with PMA/ionomycin for 4 h, surface-stained with anti-CD4, and intracellularly stained with anti-IFN-γ and anti-IL-17 and analyzed by flow cytometry.

Treatment of BMDMs with mitomycin C

For mitomycin C treatment, BMDMs from WT and *Cblb*$^{-/-}$ mice were suspended at a concentration of 2×10^7 cells/ml in PBS, and treated with or without Mitomycin C (50 μg/mL) at 37°C for 20 min. WT and *Cblb*$^{-/-}$ BMDMs with or without Mitomycin C treatment were co-cultured with 2D2 $CD4^+$ T cells in the presence of MOG_{35-55} as described above.

Determination of IL-6-producing cells by flow cytometry

WT and *Cblb*$^{-/-}$ mice were immunized with MOG_{35-55} in CFA. dLN cells were collected on day 8, and re-stimulated with PMA/ionomycin. Cells were then collected, washed, and resuspended in staining buffer (1% BSA in PBS). The cells were incubated with mAbs to various cell-surface markers for 30 min at 4°C. After washing twice with staining buffer, cells were fixed and permeabilized using Cytofix/Cytoperm solution (BD Bioscience) for 20 min at 4°C. Cells were stained for intracellular IL-6 for 30 min at 4°C. IL-6-producting cells were determined by flow cytometry. Flow cytometric analysis was performed to evaluate IL-6-producing cells in macrophages ($CD11b^+F4/80^+$), DCs ($CD11b^-CD11c^+$ and $CD11b^+CD11c^+$), monocytes/neutrophils ($CD11b^+Ly6C^+Ly6G^-$/$CD11b^+Ly6C^-Ly6G^+$), $CD3^-CD19^+$ B cells, and $CD3^+CD4^+$ T cells.

In vitro Knockdown experiments

Il6 Accell siRNA or non-sense siRNA were obtained from Dharmacon. BMDMs were plated in 12 wells and transiently transfected with 2 μg of siRNAs using Lonza Nucleofector reagent according to the Manufacturer's instruction. 36 h later, cells were harvested. IL-6 expression was determined by flow cytometry.

In vivo delivery of *Il6* siRNA

In vivo delivery of siRNA was described previously (Tang et al., 2020; Xiao et al., 2016) with some modifications. In brief, *Cblb*$^{-/-}$ mice were treated with *Il6* Accell siRNA (L-043739-00-0005, Dharmanon) at 10 nM/kg/mouse) or a non-sense siRNA by tail vein injection one day before immunization (Day −1) with MOG_{35-55} in CFA, and then twice (Day 3 and Day 7) after immunization. The *Il6 Accell* siRNA and non-sense siRNA were dissolved by sterile PBS, and the final dose of injection is 100 μL per mouse. In a parallel experiment, the dLNs from *Cblb*$^{-/-}$ mice received *Il6* Accell siRNA or the control siRNA were collected at day 10. The cells were surface-stained with anti-CD4,anti-CD11B, anti-F4/80,and intracellularly stained with anti- IFN-γ or anti-IL-17、anti- IL-6, anti- IFN-γ or anti-IL-17. The expression of $CD4^+$IFN-γ^+, $CD4^+$IL-17^+, and $CD11b^+F4/80^+$IL-6^+ populations was determined by flow cytometry.

Isolation of CNS infiltrating cells

Spinal cord was removed by insufflation using 20 mL 4°C RPMI expressed through a 19G needle. The spinal cord was transferred to 10 mL fresh, cold RPMI and homogenized by using the 5 mL syringe. Cells were pelleted by centrifugation at 300×g for 5 min at 4°C and the supernatant was discarded. The cells were resuspended in 1 mL digestion solution (PBS with Calcium and Magnesium, 1.5 mg/mL Collagenase II, 50 μg/mL DNase I) by using vortexer and incubated for 30 min, 37°C in water bath. 30–70% colloid Percoll was used to isolate CNS infiltrating cells. The cells were carefully harvested from the interphase 30–70% Percoll fraction and were transferred into new 15 mL Falcon tube containing 8mL PBS/FCS. Cells were pelleted by centrifugation at 900×g, 5 min, 4°C and the supernatant was discarded. The isolated cells were further used for detection of IL-6-producing macrophages, neutrophils, and microglia.

QUANTIFICATION AND STATISTICAL ANALYSIS

Data analysis and statistical analysis

GraphPad Prism Software (San Diego, CA, USA) was utilized for statistical analysis. A two-tailed Student's t-test was applied for statistical comparison of two groups or, where appropriate and a Mann-Whitney U test for nonparametric data (EAE scoring). Differences were considered significant at $p < 0.05$. No animals were excluded from the analysis. Mice were allocated to experimental groups based on their genotypes and were randomized within their sex- and age-matched groups. No statistical method was used to predetermine sample size. It was assumed that normal variance occurs between the experimental groups.